Journal of Materials Science and Engineering with Advanced Technology
Volume 14, Number 1, 2016, Pages 1-17
Available at http://scientificadvances.co.in
DOI: http://dx.doi.org/10.18642/jmseat_7100121665

TEMPERATURE EFFECT ON THE ELECTRONIC TRANSFER MECHANISM BETWEEN InAs/GaAs QUANTUM DOTS BY THE MEAN OF TIME RESOLVED PHOTOLUMINESCENCE SPECTROSCOPY

Z. ZAABOUB[1], F. HASSEN[1,2], M. NAFFOUTI[1] and H. MAAREF[1]

[1]Laboratoire de Micro-Optoélectronique et Nanostructures
Faculté des Sciences de Monastir
Université de Monastir
Avenue de l'environnement
5019 Monastir
Tunisia

[2]Department of Physics
College of Science
King Khalid University of ABHA
Al-Guraigar, ABHA
Kingdom of Saudi Arabia
e-mail: fohassen@kku.edu.sa

Abstract

We report an investigation of carrier dynamics in multi-layer of *p*-doped InAs quantum dots (QDs) structure grown by molecular beam epitaxy on GaAs (001) substrate. We have studied the temperature effect, the density of excitation, and the detection's wavelength effects on the decay time of the photo-generated

Keywords and phrases: InAs QDs, decay time, tunneling effects, recombination process, carrier transfer.
Received May 4, 2016

carrier. The decay time, the full width at half maximum, and the integrated photoluminescence intensity behaviours show three domains of temperature dependence. These domains are related to the carrier transfer processes between distributions of QDs of the same layer. It is shown that, at low temperature, the transfer is mainly ensured by tunneling, where the recombination process is found to be pure radiative. At the intermediate temperature, there is a competition between radiative and non-radiative recombination processes. And for high temperature, the transfer is assisted by the thermal activation and recombination is purely non-radiative.

1. Introduction

The growing need for high performance of optoelectronic devices promotes an important interest for zero-dimensional semi-conductor hetero structures. In these systems, the strong localization of the carrier wave function leads to an atomic-like electronic density of states. This property leads to the possible development and realization of novel and improved photonic and electronic devices [1]. Many properties had been optimized depending on the appropriate application. These properties are related to the stacking and vertically alignment of quantum dots for quantum computing [2], to the doping control for infrared detectors [3], lateral coupling for solar cells and tunneling diode, … etc. Recently, modulation *p*-doped self assembled quantum dots (QDs) have found important applications, such as infrared detectors [3], single electron transistors [4], memory devices [5], and lasers. Especially, for *p*-doped laser's structures, a better temperature characteristics and high-speed properties have been reported. The first feature is attributed to opposing the effect of a thermal smearing of holes in closely spaced levels [6]. The second feature is that, the high-speed characteristics of QDs lasers are known to be significantly affected by carrier capture and relaxation. In doped QD structures, the presence of built-in carriers should alter the dynamics and lead to an enhancement carrier relaxation rate.

Due to these potential applications, several studies of carriers' dynamics in modulation-doped QD structures have been reported. Siegert et al. [7] had studied the photo excited carrier dynamics in *n* and *p* modulation-doped InAs QDs by time-resolved photoluminescence

spectroscopy. For the doped samples, the presence of built-in carriers in the dots leads to an efficient electron-hole scattering, whereas in the undoped structure, scattering by phonons is identified as the main relaxation channel. They also showed a decreased of the carrier lifetimes in the doped structures, which is attributed to non-radiative recombination centers related to the dopant. From resonant photoluminescence experiments, Guasch et al. [8] concluded completely on different relaxation mechanisms for doped and undoped structures. The time resolved photoluminescence (RTPL) studies on both *n* and *p*-doped dots were reported by Gündoğdu et al. [9]. Carrier relaxation in these structures was found to be extremely fast, especially in the *p*-doped sample, which is attributed to the efficient of electron-hole scattering [10]. However, authors had studied only the carrier transfer from the barrier to the ground state of the dots without addressing details of the carrier transfer between QDs them self and its effect on the PL decay. Till now, the recombination paths and relaxations processes are not clear in QDs structures. Thus, more investigation of to understand the carriers dynamics in modulation *p*-doped QDs structure is of an importance.

To understand the electronic dynamics in InAs QDs, we have investigated the time resolved photoluminescence of a *p*-doped quantum dots stacked structure. In this paper, we will present the temperature effect on the optical properties of stacked *p*-QDs. The density of excitation and the detection wavelength effects on the decay time will be presented and discussed. The decay time, the full width at half maximum, and the integrated photoluminescence intensity behaviours show three domains of temperature dependence. These domains are related to the carrier transfer processes between distributions of QDs. It is shown that, at low temperature, the transfer is mainly ensured by tunneling and the recombination is pure radiative. For the intermediate temperature, there is a competition between radiative and non-radiative recombination, whereas for high temperature the transfer is assisted by the thermal activation and recombination is purely non-radiative.

2. Sample Design and Experimental Set-Up

The sample was grown by molecular beam epitaxy on a GaAs (001) substrate [11]. It is constituted of 30 planes of self-assembled InAs QDs, separated by 38nm thick GaAs spacer layers. The QD surface density is estimated to be 10^{10}cm^{-2}. The structure was *p*-modulation doped by carbon. A delta-doped layer is introduced in each spacer at 2nm below the QDs with a nominal density of $2\times10^{11}\text{cm}^{-2}$.

For the continuous wavelength photoluminescence (cw-PL) measurements, the sample is excited by the 514.5nm line of an Ar+ laser and the emission is detected by an In GaAs photodetector using a conventional lock-in technique. TRPL measurements were performed by using a mode-locked Ti:sapphire laser with a duration pulses of 3.5ps and a repetition rate of 80MHz operating at 780nm. TRPL detections were performed by using a Time Correlated Single Photon Counting (TCSPC) technique based on the Time Harp 200 electronic card from Pico Quant. For all measurements, the sample is mounted on the cold finger of a closed-cycle helium cryostat (10-300K).

3. Results and Discussions

The low temperature, 10K, cw-PL spectrum of the InAs QDs, measured at lower excitation power density is shown in Figure 1. The emission peak is located at 928nm (1.329eV) with a full width at half maximum (FWHM) of 28meV. No significant change in the peak's shape is observed versus the density of excitation.

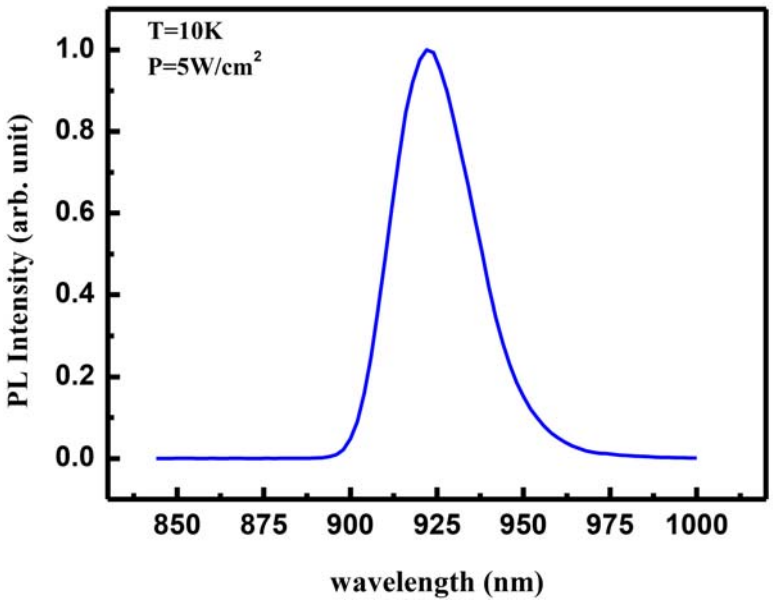

Figure 1. Normalized PL spectra of InAs QDs measured at 10K and at an excitation density of 5W/cm^2.

The integrated cw-PL intensity as a function of the temperature is plotted in Figure 2 and no remarkable change can be observed up to 100K. This is due to the fact that thermal energy is not large enough to eject carriers outside all quantum dots. This behaviour could be attributed to an effectual carrier transfer from smaller to larger dots via the tunneling path [12, 13]. By further increasing temperature, a decrease of the PL intensity is observed. This effect is due to the thermal activation of carriers localized in QDs to the wetting layer and barrier.

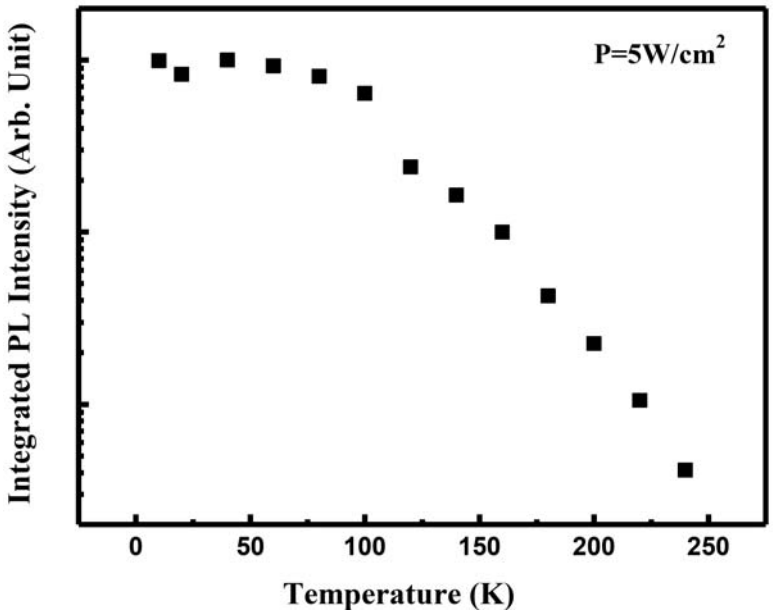

Figure 2. Integrated PL intensity as a function of temperature, measured at an excitation density of $5\mathrm{W/cm}^2$.

Figure 3 shows the temperature dependence of the PL peak energies (Figure 3(a)) and the full width at half maximum (Figure 3(b)). In these figures mainly two temperature domains are observed. For temperature less than 100K, the PL peak energy shift is well fitted by a Varshni law with a red shift of 18meV. By the same occasion the FWHM shows a minimum, located at 60K. This is due to, an effective thermal redistribution of carrier among different QDs distributions [14, 15]. For temperature higher than 100K, the FWHM shows a continuous increase [16, 17]. This behaviour is attributed to the thermal activation of carriers outside of the QDs toward wetting layer and/or GaAs barrier and interaction with phonons. This increase in the FWHM is accompanied by a second red shift of the PL emission energy (Figure 3(a)) also is fitted by a new Varshni curve. The kink in the experimental data, located nearly at 100K, and separating the two Varshni domains, is a signature of the existence of two QD's distributions.

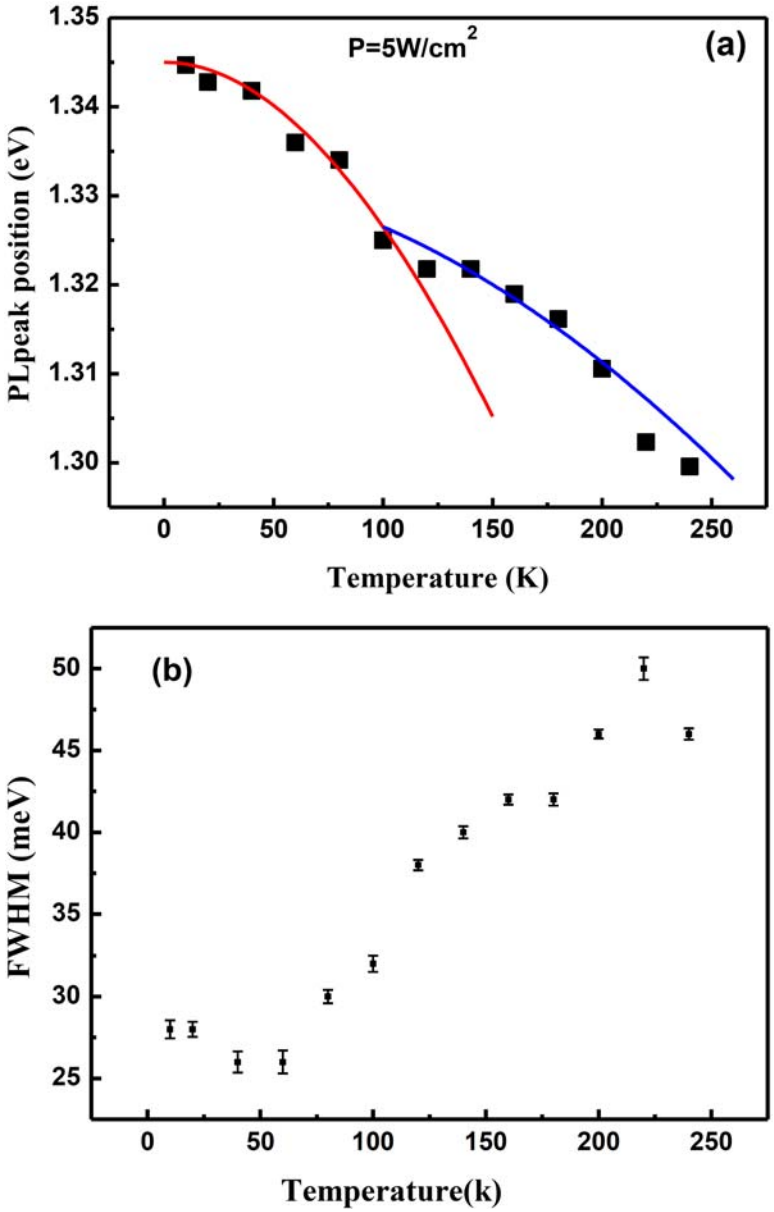

Figure 3. Temperature dependence of: (a) the PL peak emission energies, the solid curves are the theoretical Varshni's fit and (b) the full width at half maximum (FWHM).

The temperature dependence of the cw-PL peak positions and its integrated intensity provide the evidence that the carriers in QDs are strongly localized at temperatures up to 100K. To better understand these observed effects, further studies by time-resolved photoluminescence spectroscopy had been carried out, and presented in the next section.

Carrier lifetimes as a function of temperature were investigated in order to understand the carrier dynamics and recombination processes in the InAs QDs. Figure 4(a) shows the PL decay time, measured at the maximum of the PL peak, as function of the sample temperature, for a density of excitation about $440\mu j/cm^{-2}$. It can be seen that the PL decay time decreases quickly from 1.32ns to 0.700ns with increasing temperature from 10K to 100K. This variation corresponds to a ratio of 6.8ps/K. By further increasing the temperature, no remarkable change in the decay time is observed until 200K. For temperature higher than 200K, a slow decrease with a ratio of 0.7ps/K can be observed.

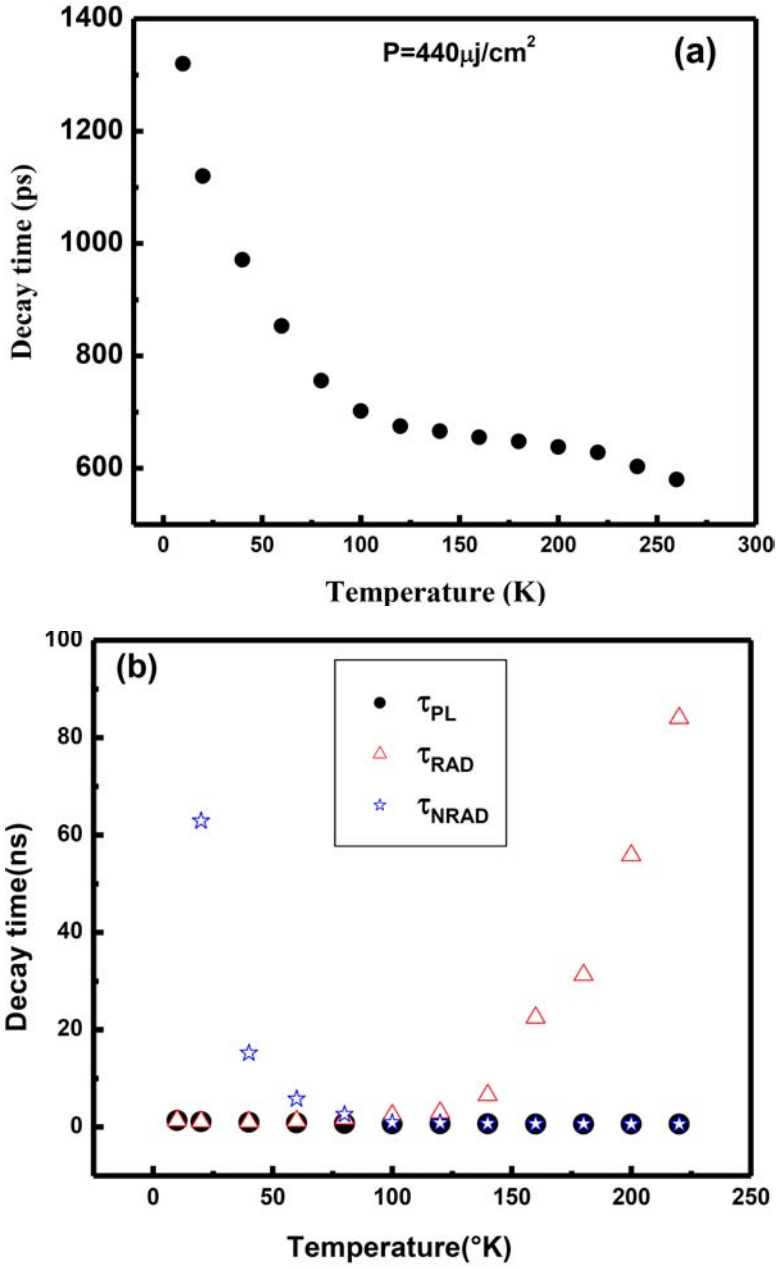

Figure 4. Temperature dependence of: (a) the PL decay time measured at the PL peak emission (928nm) and (b) the radiative and non-radiative lifetimes calculated from Equation (1) and Equation (2).

However, similar study of temperature dependence of the PL decay time profiles has been reported by Kojima et al. [18] and in [20] on undoped multilayer InAs QDs samples with 30 periods, grown by solid-source molecular beam epitaxy. Author have shown that the PL decay time is almost constant in the low temperature. This typical result was attributed to the localization of excitons in the quantum dots. At high temperature, they explain their results by the thermal dissociation of excitons and free carriers ejection from QDs to the wetting layers and barriers. On the other hand, they include another factor, namely, the effect of the vertical overlapping of the electronic wave functions, to explain the large increase of the PL decay time with increasing temperature in InAs QDs layers. In our case and contrary to these results, the interpretation of the decrease in the PL decay time as a function of temperature should exclude the vertical coupling effect of QD stacks, since our spacer is about 38nm, greater than the exciton radius. We must also emphasize that, our QDs are intentionally modulation delta *p*-doped. In fact, it has been demonstrated that *p*-doping is found to reduce the effects of hole escape, which is expected to be more widespread than electron escape. Consequently, the presence of a large number of holes in the QD will enable faster carrier relaxation processes reducing the electron relaxation time by increasing the non-radiative recombination on localized recombination centers introduced by the doping [10]. The carrier lifetime decrease can also be attributed to an enhancement of the Auger-type recombination due to the presence of extrinsic holes in the QDs [7].

The integrated PL intensity and PL decay time observed behaviours, are related to the competition between radiative and non-radiative processes. In general, the PL decay rate is given by

$$\frac{1}{\tau_{PL}(T)} = \frac{1}{\tau_{rad}(T)} + \frac{1}{\tau_{nrad}(T)}, \tag{1}$$

where $\tau_{rad}(T)$ and $\tau_{nrad}(T)$ are the radiative and the non-radiative lifetimes, respectively. Their values, at a given temperature, could be

extracted from the measured PL decay time and the integrated PL intensities by using the cw-PL data [21]. Assuming that, at low temperature the recombination is pure radiative, leading to an internal quantum efficiency $\eta = 1$ at 10K and for a temperature T is given by the simple relation $\eta(T) = \frac{\tau_{PL}(T)}{\tau_{rad}(T)} \approx \frac{I_{PL}(T)}{I_0}$. From these assumptions, one can determine the following equations [10]:

$$\tau_{rad}(T) = \frac{I_0}{I_{PL}(T)} \tau_{PL}(T), \tag{2}$$

and

$$\tau_{nrad}(T) = \frac{I_0}{I_0 - I_{PL}(T)} \tau_{PL}(T), \tag{3}$$

where $\tau_{PL}(T)$ and $I_{PL}(T)$ are the PL decay time and the integrated PL intensity, respectively, at a temperature T. I_0 is the integrated PL intensity at a sufficiently low temperature value (10K in our case).

If we assume that both radiative and non-radiative recombination processes can occur at the lowest temperature, we will obtain $\tau_{rad}(T)$ and $\tau_{nrad}(T)$ at each temperature by using Equation (1), Equation (2) and the experimental data from $I_{PL}(T)$ and $\tau_{PL}(T)$. Figure 4(b) shows the temperature evolution of the radiative, non-radiative recombination lifetimes and the photoluminescence decay time. In this figure, we can distinguish three regions, low, medium, and high temperature. In the low temperature region, the PL decay time is dominated by the radiative component, whereas the high temperature region is dominated by the non-radiative one. The medium temperature region is characterized by a competition of these two processes. From these results, we can consider that the recombination process, in the stacked QD structure, is radiatively up to 140K.

Since the sample is *p*-doped, to study the relationship between the photo-generated electrons density and the PL decay time, we have investigated the effect of the excitation density. In this section, the wavelength detection is fixed at the maximum of the cw-PL emission corresponding to 928nm. Figure 5(a) shows a selected typical PL transient with different excitation power and Figure 5(b) shows the PL decay times as function of the excitation power at 10K. For three decades of excitation density, Figure 5(a), a clear variation of the decay is observed and single exponential is used to fit each spectrum. This indicates that the PL transients at excitation density up to $1760\mu j/cm^2$ were governed by recombination on the ground-state [22]. For more detail, we have plotted in Figure 5(b), the PL decay time versus the density of excitation. A monotonic decrease with increasing the excitation density from $1.7\mu j/cm^2$ to $1760\mu j/cm^2$ is observed. In the low excitation density regime, one electron or less per QD, a large PL decay time of 1.3ns is obtained, followed by a rapid decrease with increasing the excitation power density. This behaviour is a signature of the progressive filling of the ground state for each QD. This result is supported by the effect that the decay time is inversely proportional to the carrier density [24].

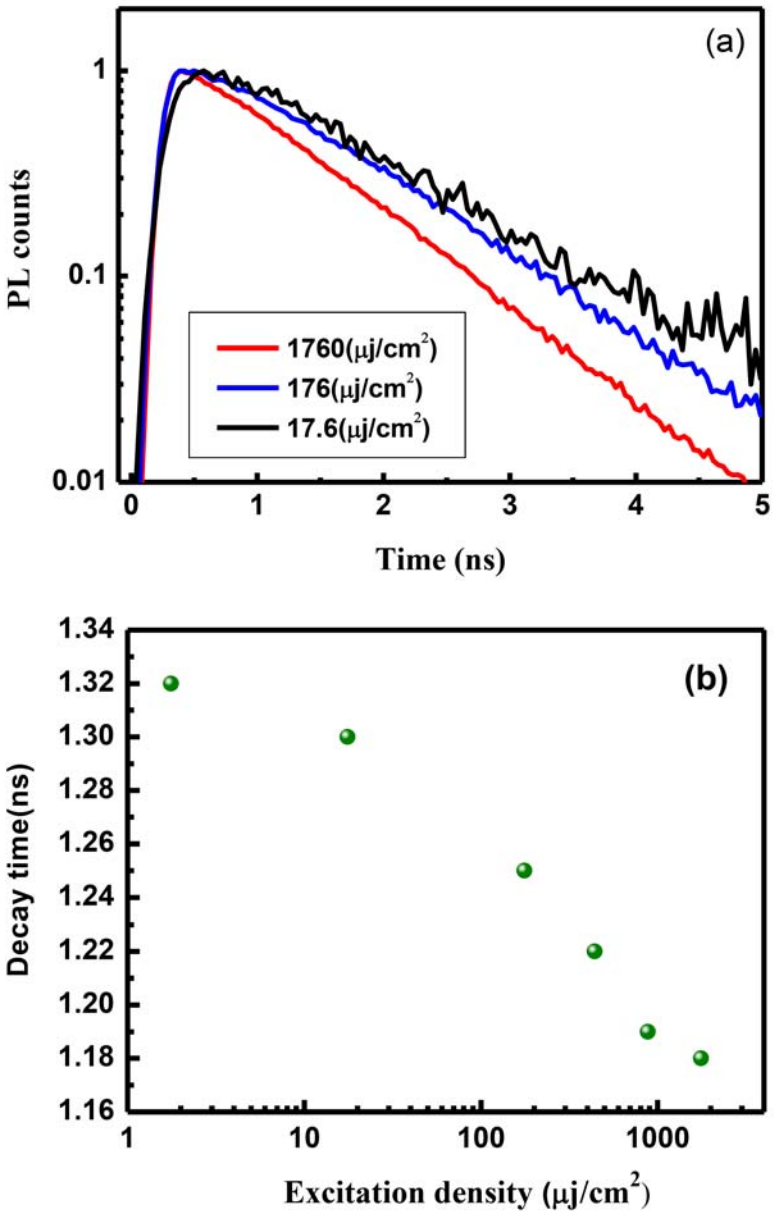

Figure 5. (a) PL decay curves acquired at the maximum of the PL peak as a function of excitation power density and 10K, (b) the evolution of the decay time as function of excitation power density.

Similar studies of the carrier density effect on PL decay time have been reported by Karachinsky et al. [23] on InAs QD single layer array. They have shown a slow decrease of the decay time (from 1.2 to 1ns) at relatively high excitation power regime. They had explained this behaviour by the filling of excited states and/or adjacent regions, such as wetting layer and barriers [22, 23]. However, the rapid decrease of the PL decay time in our QD structure, could be justified by the *p*-delta doping and multi-stacks structure, where the ground state can be saturated at low density of excitation.

To more understand the carriers relaxations and their transfer between quantum, we have studied the decay time versus the wavelength detection. As shown in the Figure 6, at low temperature, 10K, an increase of the decay time is observed when the detection is driven from low to high wavelengths. This behaviour is the result of the electronic transfer process from small to big quantum dots. This phenomenon had been observed in GaAsN microstructures [25, 26] and had been attributed to the excitonic transfer by hopping between localized states. In our sample, the decay time dispersion is due to the fact that, in small QDs, the carrier wave functions are spread through the barrier [21] leading to a an important electronic transfer toward the dig QDs by tunneling path. By increasing the temperature, photo-generated carriers will be thermally ejected out of small QDs and recombine elsewhere, leading to a reduction in the decay time dispersion [27]. At high temperature, more than 160K, the decay time tends to a constant value of 0.6ns. This means that, at high temperature, the small QDs are empty and the emission is purely from large ones, acting as traps. These assumptions are in a good agreement with that observe in cw-PL.

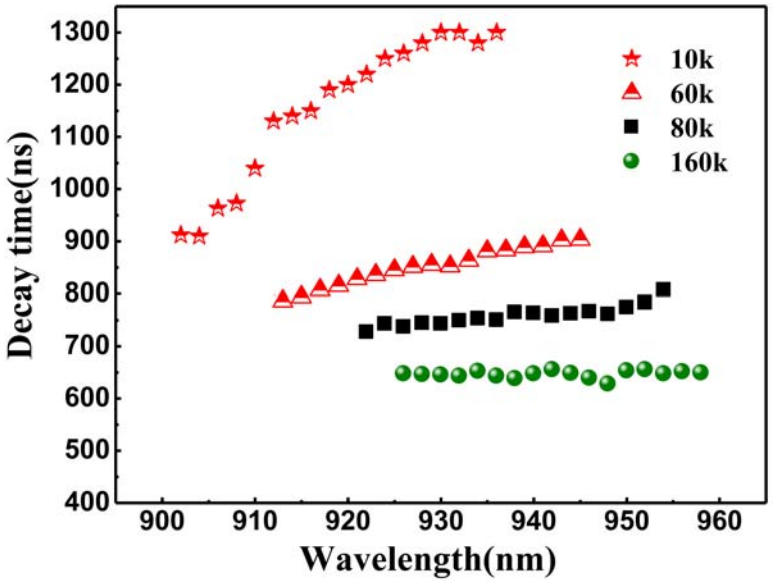

Figure 6. PL decay time as a function of the detection wavelength for different temperatures.

It is worth mentioning that the decay time dependence on temperature and QDs size is well supported by temperature dependence of the PL peak position and the FWHM. At low temperature, the photoluminescence is originated from different InAs QDs sizes. Hence, significant change of the decay time, which is dominated by the radiative lifetime, versus emission wavelength being obtained. For higher temperatures, the decay time, dominated by the non-radiative component, is insensitive to the QDs sizes. Indeed, these processes are generally governed by the recombination through the Auger path [7, 28] and recombination centers introduced by the doping [10].

4. Conclusion

In conclusion, carrier dynamics in stacked *p*-delta doped InAs quantum dots have been investigated by using cw and time-resolved photoluminescence versus the sample temperature and wavelength detection. Even in cw-PL or TRPL, we have shown the presence of three

temperature domains. At low domain, less than 60K, the recombination processes are purely radiative and electrons in small dots could be transferred to large ones by lateral tunneling. In the medium temperature region, we have a completion between the radiative and non-radiative recombination assumed by the reduction of the tunneling effect and an increase on the thermal ejection of carriers out of small QDs. At high temperature, the photo-generated carriers will be ejected out even from big QDs and recombine elsewhere, leading to a reduced decay time and insensitive the detection wavelength.

References

[1] M. Razeghi, Ebook of Electronic Materials and Devices Series, "The MOCVD Challenge: A survey of GaInAsP-InP and GaInAsP-GaAs for photonic and electronic device applications" (2011).

[2] T. Mano, R. Notzel, G. J. Hamhuis, T. J. Eijkemans and J. H. Wolter, J. Appl. Phys. 95 (2009), 109.

[3] E. Towe and D. Pan, IEEE J. Sel. Top. Quantum Electron 6 (2000), 407.

[4] S. Tarucha, D. G. Austing and T. Honda, Superlattices and Microstructures 18 (1995), 121.

[5] E. Beham, M. Betz, S. Trumm, M. Kroutvar, Y. Ducommun, H. J. Krenner, M. Bichler, A. Leitenstorfer, J. J. Finley, A. Zrenner and G. Abstreiter, Phys. Status Solidi C 1 (2004), 2131.

[6] O. B. Shchekin and D. G. Deppe, Appl. Phys. Lett. 80 (2002), 3277.

[7] J. Siegert, S. Marcinkevièius and Q. X. Zhao, Phys. Rev. B 72 (2005), 085316.

[8] C. Guasch, C. M. Sotomayor Torres, N. N. Ledentsov, D. Bimberg, V. M. Ustinov and P. S. Kop'ev, Superlattices and Microstructures 21 (1997), 509.

[9] K. Gündoğdu, K. C. Hall, Thomas F. Boggess, D. G. Deppe and O. B. Shchekin, Appl. Phys. Lett. 85 (2004), 4570.

[10] K. Gündoğdu, K. C. Hall, E. J. Koerperick, C. E. Pryor, M. E. Flatté, Thomas F. Boggess, O. B. Shchekin and D. G. Deppe, Applied Physics Letters 86 (2005), 113111.

[11] B. Eble, C. Testelin, P. Desfonds, F. Bernardot, A. Balocchi, T. Amand, A. Miard, A. Lemaýtre, X. Marie and M. Chamarro, Phys. Rev. Lett. 102 (2009), 146601.

[12] S. Sanguinetti, M. Henini, M. Grassi, M. Capizzi, P. Frigeri and S. Franchi, Phys. Rev. B 60 (1999), 11.

[13] K. Lee, B. Jo, C. Lee, I. H Lee, J. S. Kim, D. K. Oh, S. J. Lee, S. K. Noh, J.-Y. Leem and M. Y. Ryu, J. Appl. Phys. 109 (2011), 113505.

[14] Z. Y. Xu, Z. D. Lu, X. P. Yang, Z. L. Yuan, B. Z. Zheng and J. Z. Xu, Phys. Rev. B 54 (1996), 11528.

[15] Y. T. Dai, J. C. Fan, Y. F. Chen, R. M. Lin, S. C. Lee and H. H. Lin, J. Appl. Phys. 82 (1997), 4489.

[16] A. Polimeni, A. Patane, M. Henini, L. Eaves and P. C. Main, Phys. Rev. B 59 (1998), 5064.

[17] M. Grundmann, J. Christen, N. N. Ledentsov, J. Bohrer, D. Bimberg, S. S. Rumimov, P. Werner, U. Richter, U. Gosele, J. Heydenreich, V. M. Ustinov, A. Yu. Egorov, A. E. Zhukov, P. S. Kop'ev and Zh. I. Alferov, Phys. Rev. Lett. 74 (1995), 4043.

[18] O. Kojima, Chapter 10 Exciton Dynamics in High Density Quantum Dot Ensembles Finger prints in the Optical and Transport Properties of Quantum Dots Edited by Ameenah Al-Ahmadi, (2012).

[19] G. Wang, S. Fafard, D. Leonard, J. E. Bowers, J. L. Merz and P. M. Petroff, Appl. Phys. Lett. 64 (1994), 2815.

[20] R. Hostein, A. Michon, G. Beaudoin, N. Gogneau, G. Patriache, J. Y. Marzin, I. Robert-Philip, I. Sagnes and A. Beveratos, Appl. Phys. Lett. 93 (2008), 073106.

[21] H. J. Lee, M.-Yi Ryu and J. Kim, J. Appl. Phys. 108 (2010), 093521.

[22] J. W. Tomm, V. Petrov, G. G. Tarasov, H. Kissel, C. Walther, Ya. Zhuchenko and W. T. Masselink, Appl. Phys. Lett. 78 (2001), 3214.

[23] L. Y. Karachinsky, S. Pellegrini, G. S. Buller, A. S. Shkolink, N. Y. Gordeev, V. P. Evtikhiev and V. B. Novikov, Appl. Phys. Lett. 84 (2004), 7.

[24] Jasprit Singh, University of Michigan, Electronic and Optoelectronic Properties of Semiconductor Structures, Cambridge University Press 2003, ISBN-10 0-521-82379x.

[25] X. D. luo, Z. Y. Xu, W. K. Ge, Z. Pan, L. H. Li and Y. W. Lin, Appl. Phys. Lett. 79 (2001), 958.

[26] M. Baranowski, R. Kudrawiec, J. Misiewicz and M. Hammar, Appl. Phys. A 118 (2015), 479.

[27] Y. Shoji, K. Narahara, H. Tanaka, T. Kita, K. Aki moto and Y. Okada, J. Appl. Phys. 111 (2012), 074305.

[28] Y. D. Jang, T. J. Badcock, D. J. Mowbray, M. S. Skolnick, J. Park, D. Lee, H. Y. Liu, M. Hopkinson, R. A. Hogg and A. D. Andreev, Appl. Phys. Lett. 93 (2008), 101903.

■